GEOCHEMISTRY OF THE EPITHERMAL DICKITE (NOWA RUDA, LOWER SILESIA, POLAND): VANADIUM AND CHROMIUM

Pavle I. Premović[1*], Thierry Allard[2], Justyna Ciesielczuk[3], Nikola D. Nikolić[1] and Mirjana S. Pavlović[4]

[1]Laboratory for Geochemistry, Cosmochemistry & Astrochemistry, University of Niš, Niš, Serbia

[2] Institut de Mineralogie et Physique des Milieux Condensés, Université Pierre et Marie Curie, Paris, France

[3]Department of General Geology, Faculty of Earth Sciences, University of Silesia, Sosnowiec, Poland

[4]Institute of Nuclear Sciences Vinča, Beograd, Serbia

Running title: V and Cr in the Nowa Ruda dickite

[*] Corresponding author. Address: Faculty of Sciences, Visegradska 33, P.O. Box 224, 18000 Nis, Serbia.
e-mail:pavle.premovic@yahoo.com

ABSTRACT

Geochemical analyses for trace V and Cr have been made on a representative sample of a typical dickite/kaolinite filling vein at Nowa Ruda. The mineralogy of the sample is comparatively simple, dickite being the principal component (ca. 91% of total sample). Geochemical fractionation and inductively coupled plasma-optical emission spectrometry (ICP-OES) indicate that most (>90% of total metal) of V and Cr reside in the dickite. Electron spin resonance (ESR) shows that most (>70%) of V in the dickite structure is in the form of vanadyl (VO^{2+}) ions. A high concentration of Cr^{3+} is also detected in this structure by ESR. The combination of geochemical and spectroscopic tools applied on VO^{2+} and Cr^{3+} allow one to specify the Eh (>0.4 V, highly oxidizing) and pH (≤4.0, highly acidic) of the solution during the formation of dickite from the Nowa Ruda Basin.

Substantial proportions of V and Cr (as well as VO^{2+} and Cr^{3+}) in the dickite matrix were probably contained in an original hydrothermal (acid-sulfate) solution which were diluted by mixing with a groundwater, forming an epithermal solution. We suggest that hot hydrothermal fluid leached the surrounding varieties of gabbroids (diallage gabbros, olivine gabbros, troctolites and plagioclasites) enriched in V and Cr for the dickite-forming epithermal solution.

Key Words – Chromium, Dickite, Kaolinite, Vanadium.

INTRODUCTION

Most hydrothermal systems can be categorized as neutral-chloride (pH 6.4-9.6) or acid-sulfate (pH 2.2-3.1) (Nicholson, 1993). The neutral-chloride type is typical of high temperature systems (usually 573-623 K) in areas with an abundant supply of water. If these waters are significantly more acidic than pH 2, a magmatic gas contribution is likely, and the acid-sulfate water immediately attacks the surrounding rocks (Izguerdo *et al*., 2000).

As the availability of water declines, neutral-chloride systems evolve into acid-sulfate systems dominated by vapor transport. In these systems, deep neutral-chloride waters provide a source of steam, which condenses in the near-surface environment to form an acid-sulfate fluid from oxidation of H_2S to SO_4^{2-} by air oxygen (O_2). O_2 is brought to the subsurface (≤100 m depth) by meteoric water. The occurrence of sulfate ions (*i.e*., sulfuric acid) in the hydrothermal systems may also notably enhance the alteration of superficial rocks (advance argilic alteration such as dickitization) through geochemical metamorphism (metasomatosis).

The kaolinite group minerals include kaolinite, dickite, nacrite and halloysite. Acid alteration in magmatic hydrothermal systems formed by contact with acid-sulfate (SO_4^{2-}) solutions is often represented by minerals such as kaolinite and dickite (Izquierdo *et al*., 2000, and references therein). Hydrothermal kaolinite and dickite are mainly formed in situ through alteration of source minerals (mainly K-rich feldspars and other aluminosilicates) by hydrothermal acid waters and at temperatures <400 K *i.e*., under epithermal conditions (Murray *et a1*., 1993; Malengreau *et al.*, 1994). Geochemical models of diagenesis indicate that authigenic kaolinite and dickite may become unstable at moderate temperatures of about 400-420 K since they react further with K-rich feldspars to form illite (Ehrenberg and Nadeau, 1989).

Dickite is a high–temperature form of kaolinite (Schroeder and Hays, 1967); usually the dickitization of kaolinite occurs between about 373-400 K (Ehrenberg *et al.*, 1993). A geochemical study of kaolinite filling veins in Cretaceous shales from Gibraltar (Spain) showed that mean temperatures <353 K can be estimated for kaolinite mineral formation where kaolinite and dickite coexist, while temperatures on the order of 353-373 K are suitable where dickite is the sole polymorph present (Ruiz and Reyes, 1998).

The oxidation states of vanadium in the geosphere correspond to V^{3+}, V^{4+} and V^{5+}. Vanadium is present in natural waters, where redox conditions, pH, adsorption and complexation are the main controlling parameters of the solubility of this transition metal element. In oxygenated natural waters, V is predicted to occur in the +5 oxidation state, primarily as highly soluble and mobile vanadate ions: $H_nVO_4^{n-3}$ (n=0 to 4), and as $NaHVO_4^-$ (Turner *et al.*, 1981). As a consequence, the V species involved in incorporation processes appear anionic, resulting in a relatively low affinity for the negatively charged colloidal clay particles (Whitfield and Turner, 1987). Vanadyl ion (VO^{2+}) shows a strong tendency to interact with the surface of Al and other metal hydrous oxides and is thus capable of becoming specifically bound within the colloidal clay particles (Wehrli and Stumm, 1989).

Geochemical studies indicate that Cr occurs in natural aquatic environments in two oxidation states: Cr(III) and Cr(VI). In low (suboxic/anoxic) Eh natural environments, the main aqueous Cr(III) species are Cr^{3+} and $Cr(OH)^{2+}$. Under oxidizing conditions, aqueous Cr is present in a Cr(VI) anionic form, $HCrO_4^-$ and/or CrO_4^{2-}, depending on the pH. Cationic Cr(III) species are rapidly and strongly adsorbed by colloidal clay particles, but adsorption of anionic Cr(VI) species onto these particles is expected to be minimal (Rai *et al.*, 1986, 1987).

The conditions of formation of hydrothermal kaolinite/dickite are rarely studied, although the metal species hosted in their structure can be used as proxies. As a matter of fact, VO^{2+} and Cr^{3+} in natural aquatic environments are characterized almost entirely by the pH and oxidation reduction potential (Eh) of the environment. These two parameters also have a strong influence on the mobility and complexation of VO^{2+} and Cr^{3+} ions. These two ions, therefore, are sensitive geochemical indicators of the geochemistry of the clay–forming solutions and may provide clues to the origin of the clay deposits of the past. This has led us to study VO^{2+} and Cr^{3+} in dickite from Nowa Ruda (NR), a hydrothermal mineral enriched in V and Cr (Morawiecki, 1956). After a mineral characterization of the sample using X-ray diffraction and Fourier transform infrared spectroscopy, selective leaching procedures were performed to establish specific mineral hosts for V and Cr. To support the speciation study, we quantitatively determined the VO^{2+} concentration in dickite using a new experimental calibration with a principle derived from a previous study of kerogens and asphaltenes (Premović *et al.*, 2000).

EXPERIMENTAL

Geological setting

The NR Basin is located in the Sudetes Mountains (southwestern Poland), near the city of Wroclaw (Fig. 1a). The geology and mineralogy of this basin were extensively studied by Morawiecki (1956), Kowalski and Lipiarski (1973), and Borkowska (1985). The gabbro-diabasic massif of the NR Basin, which spreads over 15 km^2, is composed of rocks of probable Proterozoic age (Oberc, 1960) and is represented by olivine gabbros, olivine-free gabbros with diallage, troctolites and plagioclasites. Most of these rocks reveal postmagmatic alternation. The upper part of the gabbroic rocks is weathered.

The regolith covering the gabbroic rocks, composed mainly of bauxites, argillites, and gabbros, breccias and conglomerates, is of Carboniferous age (Wiewióra, 1967). These formations are overlain by a thick series of shales of Westphalian A age, which are followed by sandstones and carbon-bearing kaolinitic shale of the Late Carboniferous formation. The Late Carboniferous is represented by carbon-free sandstones and conglomerates and is overlain by the clastic formation of Rotliegendes. Quaternary clays, gravels and sands represent the youngest rocks. The general stratigraphic succession of NR Basin is shown in Fig. 1b.

Dickite/kaolinite occurs mainly as veins within the gabbro weathering products, or is associated with the dark-grey kaolinitic shale. The mineral is usually light green or bluish-green (Fig. 2). Apart from these veins, kaolinite at the NR location also occurs in the form of large lenses. According to Kowalski and Lipiarski (1973) kaolinite and dickite from NR Basin may have originated in the epithermal solutions genetically related to the magmatism of the Late Carboniferous.

Sample location and description

Kaolinite and dickite are found throughout the abandoned coal mine Piast near the town of NR. These minerals are generally believed to be the most common product of an epithermal alteration (Morawiecki, 1956). A representative blue dickite sample (hereafter DS) was collected by Professor L. Stoch in a vein of kaolinitic shale at the Piast mine. A similar dickite sample was also collected with by one of the authors (J. C.) from the same mine.

Analytical methods

ESR spectrometry. The ESR measurements were performed on finely-grounded powders of the dickite samples that were transferred to an ESR quartz tube. Spectra were recorded on a Bruker ESP 300E spectrometer at X-band (9.4 GHz) using standard 100 kHz field modulation. The spectra were recorded at room temperature.

Measurements were performed with calibrated silica tubes and constant filling factor of the resonance cavity. Tests verified that all spectra were obtained with instrumental parameters which gave no instrumental effects on signal height/shape/width. Most of measurements were run at 2 mT modulation amplitude, 100 ms time constant, and 16 min scan time.

Fourier Transform Infrared (FTIR) Spectrometry. FTIR spectra were recorded, in absorbance mode, with a BOMEM Michelson Series MB FTIR spectrometer set to give undeformed spectra. The resolution was 4 cm^{-1} in the 400-4000 cm^{-1} analyzed range. Spectra were obtained at room temperature from KBr pressed pellets prepared by mixing 1.5 mg of a clay sample with 150 mg of KBr.

Scanning Electron Microscope (SEM). The morphology and the semiquantitative chemical analyses were performed by scanning electron microscopy (scanning microscope Philips XL 30 ESEM/TMP) coupled to an energy-dispersive spectrometer (EDAX type Sapphire). The backscattered electron (BSE) mode was done before microprobing. Analytical conditions were as follows: accelerating voltage 15 or 20 kV, probe current 60 nA, working distance 25 mm, counting time 100 s. Individual parameters are printed on photos: acceleration of electron beam, magnification, type of detector: SE (secondary electrons), CEN (BSE-backscattered electrons). Samples were coated with gold.

X-ray Diffraction Analysis (XRD). XRD patterns were obtained with a Philips PW 1729 vertical goniometer using CoKα radiation (35 kV, 30 mA). Powder diffractograms were acquired in the 3-90^o 2θ range, with 7-20 s counting per 0.04^o 2θ step. Samples were prepared using the back-loading procedure according to Moore and Reynolds (1989), providing significant disorientation of clay layers.

Analysis and fractionation

The fractionation procedure was similar to that used by Premović (1984) and it was performed on DS only. The flow chart in Fig. 3 outlines the major steps in preparing the four fractions. These are:

Powdered dickite (1 g) was treated (room temperature, 12h) with acetate buffer: acetic acid/sodium acetate (1 M, 12h) solution at pH 5.0 to remove most of the carbonates. This solution also removes other soluble minerals. The soluble material constitutes the carbonate fraction.

The insoluble residue (I) was demineralized further by repeated treatment with cold HC1 (6 M). This acid solution removes mostly metal hydroxides and oxides, including V- and Cr-hydroxides and -oxides. Soluble part constitutes the cold HCl-fraction.

The insoluble residue (II) was demineralized with boiling HCl (6 M, 80°C, 12h). This treatment removes most of soluble silicates. The soluble part constitutes the boiling HC1- fraction.

The insoluble residue (III) was demineralized with boiling mixture of HF (22 M)/HCl (12 M) (3:1 v/v, 80°C, 12h). This acid mixture removes SiO_2 and $A1_2O_3$. SiO_2 and Al_2O_3 removal was checked by FTIR/EDS analyses. The soluble part constitutes the dickite fraction.

The final residue from (III) is the acid insoluble fraction.

RESULTS

Chemical and ICP-OES analyses

The acetate buffer/HCl demineralizing steps remove only 7% of DS. This is due to the total dissolution of carbonates and other soluble minerals [acetate buffer: 3%], the dissolution of metal hydroxides and oxides (*e.g.*, V- and Cr-hydroxides and -oxides) [cold-HC1: 1%] and the destruction of some silicate minerals [boiling HCl: 3%] (Table 1a). SiO_2 and $A1_2O_3$, the dominant constituents of dickite, seem to be unaffected by these demineralization steps. Geochemical analysis also indicates that more than 97% of the dickite fraction is removed by the HF/HCl step.

Table l shows the distributions of V and Cr among the four components of DS. These results show that the HF/HCl fraction contains >98% and <97% of the total V (175 ppm) and Cr (410 ppm), respectively, indicating that the bulk of V and Cr reside primarily within the dickite structure. In addition, acetate buffer/cold-HCl leaching removed less than 1% of total V and Cr. This result indicates that a negligible amount of V and Cr is in the form of hydroxides and/or oxides that can be specifically adsorbed on the colloidal clay particles or precipitated (Evans, 1978).

XRD analyses

XRD patterns of powdered DS showed that the predominant mineral in these rocks is dickite.

FTIR analyses

An accurate distinction between kaolinite and dickite can be achieved by using FTIR, assessing the position and relative intensities of the OH-stretching bands in the 3600 - 3700 cm^{-1} region of an FTIR spectrum (Russel, 1987). The FTIR spectrum of DS is shown in Fig. 4 and is characteristic of dickite. Dickite shows strong absorption at 3621 cm^{-1} and two medium-strong absorption bands at 3704 and 3654 cm^{-1}, whereas absorption bands for kaolinite are at 3697, 3620, 3669 and 3652 cm^{-1}. FTIR analysis also showed that dickite is the only kaolinite mineral present in DS, confirming the XRD analysis.

SEM/EDS analyses

Under the SEM, DS have the morphology of well-formed, uniform aggregates of large (≤10 μm) blocky dickite crystals (Fig. 5). EDS analyses show that this mineral mainly consists of O, Al and Si (Fig. 6); minor K, Fe and Ti were also detected. This elemental composition is indicative of minerals of kaolinite group.

ESR analyses of VO^{2+}

Two main sets of transitions can be distinguished at high magnetic field in the total ESR spectrum of untreated DS, around 3400 G and at low magnetic field around 1500 G, corresponding to VO^{2+} and Cr^{3+}, respectively (Balan *et al.*, 2002). At high magnetic fields, the untreated DS shows a multiline spectrum (Fig. 7a) similar to the spectrum of VO^{2+} ions incorporated into the lattices of some kaolinites (Premović, 1984; Muller and Calas, 1993). The spectrum shows an anisotropic spectrum pattern typical of an axially symmetric hyperfine coupling.

The method employed to quantify VO^{2+} (Premović *et al.*, 2000) is given by the following equation:

$$[C_c] = (S_c/S_{st})\ [C_{st}]$$

where C is the concentration of VO^{2+}, c indicates the clay sample and st indicates the standard. S is the specific signal intensity (the integrated area under the corresponding ESR absorption per g of the sample).

A glycerol solution was prepared by first dissolving known amounts of $VOSO_4 \times 5H_2O$ in a solution containing 1.5 mL of concentrated H_2SO_4 + 0.5 mL of deionized H_2O and then diluting it with glycerol to the desired VO^{2+} concentration (8000 ppm) with thorough agitation. Although the $VOSO_4 \times 5H_2O$ reagent (Merck) had impurity content below 10^{-5}%, the real amount of VO^{2+} ions in a weighted portion could be different from the theoretical one because of the loss of crystallization H_2O and partial oxidation of VO^{2+} ions. Therefore, just before preparing the standards, the composition of $VOSO_4 \times 5H_2O$ was checked using the most precise gravimetric/titrimetric methods of chemical analysis, providing a relative standard deviation (RSD) less than 5%.

Changes in the loading Q-factor of the ESR cavity can result in samples with different dielectric properties or surfaces. The above glycerol solution has a high dielectric constant (about 56 D) and cannot be used as a reliable comparison of relative VO^{2+} concentrations of clays. For this reason, standards were prepared by mixing/diluting small amounts of the glycerol solution with kaolinite to the desired VO^{2+} concentrations. Preparing this mixture has the effect of maintaining the dielectric medium of standards close to the clay samples, keeping the Q similar. The standards prepared in this way (using a vibrating Perkin-Elmer mill) covered the range of 50 to 400 ppm of VO^{2+}. Kaolinite used in these standards was KGa-2 (Georgia, USA), which contains very low amounts of VO^{2+} (<5 ppm).

Fig. 7 also illustrates the anisotropic ESR spectrum of: (b) an initial solution of $VOSO_4 \times 5H_2O$ compound dissolved in H_2SO_4/H_2O and diluted with glycerol and (c) a standard containing 400 ppm of VO^{2+}. These spectra are typical of those previously reported for VO^{2+} in either powder (polycrystalline) solids or extremely highly-viscous liquids (Goodman and Raynor, 1970).

Only one line of the VO^{2+} anisotropic hyperfine pattern is considered for obtaining the integrated area. Consequently, just a narrow part of the VO^{2+} spectrum needs to be recorded. For this purpose, we select the first derivative ^{51}V hyperfine line marked with $m_I = -5/2||$ in the spectra of DS (Fig. 8a) and the standard (Fig. 7c). This line was chosen in order to keep the linewidth and lineshape similar and to minimize interferences from both neighboring VO^{2+} resonance lines and the lines of other ESR active species present. In addition, from our continuing study of VO^{2+} in various clay materials, we have found that the anisotropy of the ESR parameters of VO^{2+} in various clays has little or no effect on linewidth and lineshape of the -5/2|| line.

The area under the -5/2|| line was evaluated taking into account baseline corrections, multiplying or dividing it by factors required to put the areas of the -5/2|| line of both the standards and DS on the same setting.

A study of intensity and width of standard and the DS spectra versus the square root of microwave power showed no saturation. Consequently, a high power of 100 mW was selected for measurement, ensuring a high absolute intensity of the -5/2|| line.

We also plotted the integrated area of the -5/2|| line (vs. days) for five standard samples containing 400 ppm of VO^{2+} prepared on five different days. A scatter of points was obtained averaging to a straight line (parallel to the day axis) with a deviation of <5%. The repeatability of these results was <20 ppm of VO^{2+} at the 400 ppm level. We note that the VO^{2+} standards in the present case make the method applicable to any clay sample with a VO^{2+} concentration in the range of 50 to 1000 ppm.

Although DS was not collected from freshly exposed mine faces, repeated ESR analyses over the course of several months showed no change in its VO^{2+} content, consistent with previous studies of VO^{2+} stability in kaolinite (Muller and Calas, 1993). Similar experiments on the VO^{2+} standards showed that after several weeks no oxidation had occurred. After six weeks of exposure to air the VO^{2+} concentration was virtually unchanged from its initial value.

If the specific intensities of the -5/2|| lines of the standards are simply plotted against the VO^{2+} concentration a linear calibration curve is obtained. Fig. 8 shows this plot in the 50-400 ppm range. Using this plot as the calibration curve, DS was recorded for the VO^{2+} spectrum and the specific intensity of the -5/2|| line was determined to obtain the concentration of VO^{2+}. The vanadyl concentration obtained for DS is 160 ± 20 ppm, corresponding to more than 70% total V (Table 1a).

The demineralizing steps with the acetate buffer/HCl do not affect the concentrations of the VO^{2+} ions in DS. However, VO^{2+} ions disappear (checked by ESR), completely during HCl/HF demineralization. It is reasonable to assume, therefore, that these ions are incorporated into the dickite structure. Indeed, a negligible contribution of dipolar magnetic broadening arising from interactions between VO^{2+} and the neighboring VO^{2+} and/or other V ions (as expected from the low V content of dickite, Table l) is consistent with this notion. The lack of change of the ESR signals attributed to VO^{2+}, even upon prolonged (10 h) laboratory heating of the dickite at 500 K and in the presence of air, indicates that this ion is strongly bound to the dickite structure.

ESR analyses of Cr^{3+}

The representative ESR spectrum of Cr^{3+} within the dickite lattice is shown in Fig. 9 at low magnetic field. According to Balan *et al.* (2002), the above ESR spectrum is characteristic for isolated Cr^{3+} ions in the diamagnetic matrix of the dickite structure. These authors showed that Cr^{3+} substitutes for Al^{3+} in the octahedral layer.

In the present study, we show that like VO^{2+}, Cr^{3+} is completely removed with HCl/HF demineralization. The corresponding concentration of Cr is 435 ppm. This confirms that Cr^{3+} (like VO^{2+}) ions are located within the dickite structure of DS and are probably present in a significant amounts.

DISCUSSION

Paragenesis of the hydrothermal NR dickite/kaolinite

According to Morawiecki (1956), the kaolinite minerals associated with NR veins consist only of nearly pure dickite or well ordered kaolinite. Kowalski and Lipiarski (1973) reported, however, that these veins are composed of kaolinite and dickite but in variable ratios, although dickite was the sole polymorph identified in the most veins. They suggested that there may be minerals with structures intermediate between kaolinite and dickite. The fact that dickite occurs only in parts of NR Basin indicates that the epithermal temperatures necessary for dickite formation were reached only locally. Kaolinite and dickite in NR Basin are probably genetically linked. Three parageneses of this hydrothermal kaolinite and dickite are possible: (a) kaolinite and dickite formed at the same time but at different temperatures; (b) kaolinite and dickite formed at different times from different epithermal solutions; and, (c) kaolinite formed everywhere and subsequently converted to dickite. The variable mixtures of kaolinite and dickite at a number of localities of NR Basin exclude the first two alternatives. Thus, we tentatively conclude that the low precipitation temperature of NR kaolinite was followed by dickitization. In general terms, the genesis of dickite and kaolinite in NR basin can be considered similar to that of kaolinite–filling veins in Cretaceous shales from Gibraltar (Ruiz and Reyes, 1998). Hence, we assume that the epithermal solutions in the veins of NR Basin, where kaolinite and dickite coexist, had mean temperatures about <350 K, and temperatures on the order of 350-370 K where dickite is the sole polymorph present.

As many hydrothermal systems are dominated by waters of meteoric origin (Arehart and Poulson, 2001), dickite-forming epithermal waters at NR Basin were probably ultimately meteoric. Many geochemical studies (*e.g.*, Ehrenberg *et al.*, 1993; McAulay *et al.*, 1993; Lanson *et al.*, 1996; Beaufort *et al.*, 1998; Cassagnabere *et al.*, 1999; Hassouta *et al.*, 1999) have shown that blocky dickite (such as NR dickite, Fig. 5) resulted from the diagenetic evolution of early vermiform kaolinite (as a transient intermediate) with increasing temperature rather than from a direct precipitation event induced by epithermal meteoric waters. For this reason, we tentatively suggest that kaolinite in NR Basin probably formed at shallow depths, through interaction of low temperature meteoric waters with detrital Al-rich silicates (*e.g.*, feldspars). As the temperature increases, intermediate vermiform kaolinite progressively converts to blocky dickite.

Gabbros as a source of V and Cr in NR dickite

As mentioned earlier, the hydrothermal kaolinite and dickite of NR Basin are probably related to magmatism of the Late Carboniferous period. Kraynov and Ryzhenko (1992), who made a thorough study of Eh/pH in many geochemical water types, reported that the acidity of the hydrothermal waters (in areas of contemporary magmatism) is within at pH range of ca. 0-4 and that the Eh values vary from 0.6-0.9 V. The field of these waters is marked in Fig. 10 as shaded. The epithermal solutions in NR Basin were probably acid-sulfate waters formed by a reaction of geothermal gases (mainly SO_2) with near-surface (≤100 m) oxygenated groundwater. Redox conditions in near-surface environments favor the presence of sulfur as SO_4^{2-} over H_2S. This is in good agreement with the general minor pyrite (FeS_2) association with NR dickite and kaolinite, which would otherwise indicate sulfidic (S^{2-}) conditions.

Geochemical data suggest that the geological conditions under which dickite formed must have been relatively rich in V and Cr (i.e., VO^{2+} and Cr^{3+}), and they were introduced into dickite during formation aided by an invasive epithermal solution at temperatures of 350-375 K. The fact that >95% of V and Cr (Table l) resides within the dickite structure indicates that most V and Cr in dickite-forming solution was in a dissolved form. We suggest that most of these two metals were introduced into dickite (i.e., initially into the intermediate vermiform kaolinite) by this solution already enriched in V and Cr.

An extensive geochemical study of the gabbro massifs in NR Basin was carried out by Bialowolska (1973). According to this author, V in gabbroic rocks of the basin occurs mainly in disseminated form replacing iron and is mostly concentrated in pyroxenes (300 ppm) but it is much less abundant in olivines (10 ppm). Among the NR gabbros, the highest Cr content (635 ppm) is concentrated in the olivine type. Diallage gabbros and troctolites contain about 300 ppm of Cr. Chromium occurs in disseminated form, replacing the trivalent iron in minerals according to diadochy. It also forms the own minerals, i.e. chromite and Cr-spinel associated with serpentinized pyroxenes. For this reason, we propose that hot hydrothermal fluids leached the surrounding gabbros, providing V and Cr for mineralizing epithermal solutions.

Initial hydrothermal solutions were mixed with groundwaters in NR Basin, which probably significantly decreased the concentrations of V and Cr. We believe that the final contents of V and Cr in dickite-forming solution depended less on their initial values than on the degree of subsequent mixing of these two waters. Morawiecki (1956) carried out geochemical analyses of two samples of almost pure dickite and one sample of nearly pure kaolinite from NR veins. The dickite samples (on a whole-rock basis) contained V (55 and 80 ppm) but Cr (250 ppm) was found only in one of these minerals. Such Cr discordance can only be explained in terms of the difference between the dickite-forming solutions. The fact that NR kaolinite studied by Morawiecki (1956) contained high V (430 ppm) but not Cr is in line with this interpretation. The variability in V and Cr concentrations associated with kaolinite and dickite in NR Basin probably represents a difference in dissolved V and Cr in their epithermal precipitating solutions as they were a mixture of the original hydrothermal fluid and groundwater at that time.

Conditions of formation of dickite: Eh-pH diagrams

Turekian and Wedepohl (1961) quoted the average contents of V (130 ppm) and Cr (90 ppm) of ordinary (non-hydrothermal) clays. Compared with these clays, DS (see Table l) is only slightly enriched in V and moderately (4.5 times) enriched in Cr.

As mentioned above, most V and Cr in dickite-forming solutions of DS were in a dissolved form. We assumed that the concentration of V in this solution was about 5 ppm. This assumption is based upon a content of about 5 times the V concentrations typical of natural waters, i.e., generally less than 1.2 ppm (Wanty and Goldhaber, 1992, and references therein).

In the case of Cr, a geochemical calculation suggests that all Cr would be in dissolved form if the total concentrations of Cr in the aquatic system at 300 K are lower than 7.5 ppm (Richard and Bourg, 1991). Taking into account that Cr in DS occurs in the form of metal hydroxides and/or oxides (Table 1a), Cr concentrations in dickite-forming solution of DS were probably about 7.5 ppm (i.e., $<1.5 \times 10^{-4}$ mole L^{-1}); for comparison, the concentrations of dissolved Cr typical of natural waters are <1 ppb (Richard and Bourg, 1991).

We have constructed the stability field of VO^{2+} and Cr^{3+} assuming a total V concentration of 5 ppm in aqueous solution (Fig. 10) using the FactSage thermochemical software/Fact compound databases. For the sake of simplicity, we present only a part of the diagram. The critical boundary between the stability fields of VO^{2+} and Cr^{3+} is not significantly affected by modifying this value 10-fold in either direction.

Of course, the Eh-pH diagram in Fig. 10 is not an accurate representation of the epithermal solution when dickite is formed, and it is undoubtedly highly variable in its approach to the ideal. However, because it represents a quantitative estimate based on the available thermodynamic data, it should be a helpful tool, if used within its limitation.

Fig. 10 only shows the domains of VO^{2+} and the solubility for crystalline VO_2 or V_2O_4. We note that the (hydrous) $V(OH)_2$ is probably more soluble than its anhydrous counterpart. It is apparent from this figure that the VO^{2+} ion is stable thermodynamically under oxidizing conditions ($Eh \geq 0.0$ V) only at low pH (≤ 4). Thus, the presence of relatively high concentration of VO^{2+} in NR dickite indicates that oxic dickite-forming solution was probably highly acidic ($pH \leq 4$).

The VO^{2+} stability field of the diagram is confined by superimposing the Eh-pH field for Cr^{3+} for the physicochemical conditions of dickite-forming solution (Fig. 10). It is apparent from this figure that for coexistence of VO^{2+} and Cr^{3+} during formation of dickite, the Eh values should be >0.4 V (highly oxidizing) and pH≤4.0. The VO^{2+}-Cr^{3+} domain is very close to the Eh-pH domain corresponding to modern hydrothermal waters in areas of contemporary magmatism, which are within the pH range of ca. 0-4 and Eh values of 0.6-0.9 V (Kraynov and Ryzhenko, 1992).

In much of the area of interest, the dominant dissolved species is Cr^{3+}, except above pH 4, where hydroxide complex, $CrOH^{2+}$, is a major form. A solubility of about 7.5 ppm (about 1.5×10^{-4} mole L^{-1}) for Cr could only be attained if the solid Cr species in dickite-forming solution was amorphous $Cr(OH)_3$. The anhydrous crystalline species Cr_2O_3 is much less soluble, below about 1 ppb (10^{-8} mole L^{-1}). In our opinion, the solubility of $Cr(OH)_3$ is probably more realistic for this solution.

Under the deduced oxidizing (Eh>0.0 V) and highly acidic (pH≤4) conditions, the bulk of Cr present in dickite-forming solution of DS should be present as Cr^{3+} ions, with much smaller amounts of $CrOH^{2+}$ and $Cr(OH)_2^+$. Indeed, chemical studies indicate that the Cr^{3+} ion is prevalent only at a pH lower than 3.5 and the solubility of Cr^{3+} in an aqueous solution decreases as the solution pH rises above pH 4, with essentially complete precipitation as $Cr(OH)_3$ occurring at about pH 5.5 (Richard and Bourg, 1991, and references therein). Moreover, according to reported hydrolysis constants (Rai *et al.*, 1987), Cr^{3+} is strongly hydrolyzed in aqueous solutions and the predominant species in the pH range 6.5-10.5 is $Cr(OH)_3$. Thus, the dissolution of Cr(III) minerals could only occur in natural acid waters with pH<5, giving low, equilibrium controlled, concentrations of Cr(VI) anions. For this reason, soluble Cr^{3+} is usually restricted to hydrothermal acid-sulfate waters (DeLaune *et al.*, 1998).

The V/Cr ratio has been used as a paleoenvironmental indicator of sedimentary conditions (Jones and Manning, 1994, and references therein). Values of V/Cr ≥4 are thought to represent suboxic/anoxic conditions. Values ≤4 indicate slightly oxidizing (dysoxic) conditions, with values ≤2 suggesting oxic conditions within the deposit. The V/Cr ratio of dickite is ca. 0.4 (Table la), indicating that this mineral formed in an oxidizing environment. Note that one of the NR dickite samples analyzed by Morawiecki (1956) has a V/Cr ratio of 0.2.

The abundant association goethite with NR dickite (Komusinski *et al.*, 1981) is consistent with its formation occurring under oxidizing conditions as goethite occurs only in a natural aqueous milieu under oxidizing conditions with Eh above 0.15 V (Krumbein and Garrels, 1952). In relation to this dickite, it should be noted that: (a) goethite is ultimately the most stable mineral phase associated with acid-sulfate waters (Bigham *et al.*, 1996); (b) the goethite formation becomes predominant at pH>3 (Davis *et al.*, 1988); and, (c) goethite transforms at temperatures between 420 K to 500 K (Watari *et al.*, 1983). Pyrite trace was also detected in DS but not in the dickite sample collected by J. C. and it is probably of postdiagenetic (secondary) origin.

The findings of highly oxidizing Eh values at low pH are consistent with the physicochemical characteristics of the hydrothermal (acid-sulfate) waters. Thus, dickite probably grew from an O_2–enriched acid epithermal solution at temperatures between 375 and 400 K. The epithermal solution of very low pH (≤4.0) is also consistent with an oxidizing medium, as the oxidation of H_2S to SO_4^{2-} in these waters produces a minimum pH of 2.8 (Nicholson, 1993). Laboratory synthesis in a closed system and under epithermal conditions shows that the optimal pH for kaolinite formation is 3 to 3.5 (Lahodny-Sarc *et al.*, 1993). The problem is, however, that the epithermal aquatic system of NR Basin was probably thermodynamically open, so it might not be exactly comparable to a laboratory autoclave synthesis.

The above Eh-pH diagram is calculated for atmospheric pressure and a temperature of 300 K. A thermochemical calculation indicates that no significant variations at the scale of our diagram are expected in the thermodynamic parameters up to 10 bars of atmospheric pressure. This is due to the fact that pressure only slightly affects the chemistry of both the ionic species and solids of V and Cr within the O-H geochemical system. A similar calculation also shows that in an epithermal solution with temperatures up to ca. 400 K, the vertical line (as the boundary between the VO^{2+} solution and the solid VO_2 stability field) would be shifted from pH 3.9 to 4.5. On the other hand, the vertical line, which represents the boundary between Cr^{3+} and $CrOH^{2+}$, would shift from pH 4 to 3.1. Thus, a change in the temperature up to 400 K would slightly shift the stability fields of VO^{2+} and Cr^{3+} in the Eh-pH diagram during formation of NR dickite toward a pH lower than 4.

Dickite from Jedlina Zdroj

We also investigated kaolinite mineral samples from the outcropping vein site at Jedlina Zdroj (ca. 20 km away from the Piast mine). These samples were collected by one of the authors (J. C.). All of the samples analyzed (by XRD, FTIR and SEM/EDS) contain either predominantly kaolinite or predominantly dickite, with either minor amounts or none of the complementary polytype. According to Lydka (1966), dickite from Nowa Ruda and Jedlina Zdroj dickite originated in the same epithermal episode. Geochemical data for the Jedlina Zdroj dickite are given in Table 1b.

In contrast to DS, the untreated dickite sample from Jedlina Zdroj showed only a complex ESR signal around g=4 (Fig. 11). Such an ESR pattern has been found frequently for isolated Fe^{3+} ions in a well-ordered kaolinite structure (Gaite *et al.*, 1997), substituting for Al^{3+} in octahedral sheets. These Fe^{3+} ions were resistant against chemical treatment by HCl, but after treatment by the HF/HCl solution, their ESR signals disappeared, indicating that they are probably within the dickite structure.

Other hydrothermal kaolinites and dickites

In the following, we briefly review relevant geochemical data (ours and others) for hydrothermal kaolinites and/or dickites from Sonoma (California, USA), Cigar Lake (Canada), Teslić (Bosnia and Hercegovina), Nopal (Mexico), Cornwall (England) and the Rincon de la Vieja volcano (Costa Rica).

Hydrothermal kaolinites from Sonoma. Mosser *et al.* (1996) examined two V- and Cr-bearing hydrothermal kaolinites (named MILO and GEY) that formed in an epithermal environment at Sonoma (California, USA). The Cr and V abundances in the MILO and GEY kaolinites are presented in Table 1c. These studies imply that Cr^{3+} ions are present within their structures, substituting for Al^{3+} in the octahedral sites. These authors also detected VO^{2+} (by ESR) ions in these kaolinites.

Low V/Cr ratios (≤0.1, Table 1c) for the MILO and GEY kaolinites indicate an oxygenic milieu for their formation. The fact that most of the Fe is localized in small oxide particles associated with the kaolinites (Mosser *et al.*, 1993) strongly supports this view.

Hydrothermal kaolinite of Cigar Lake. The U-rich (*ca.* 0.3%) hydrothermal deposit of Cigar Lake contains predominantly of kaolinite (>80%) and minor illite (<8%) (Mosser *et al.*, 1996). Table 1c lists the V and Cr concentrations of this kaolinite. Mosser *et al.* (1996) suggest that the Cigar Lake illite was hydrothermally transformed into kaolinite with V entering the octahedral sites.

Our ESR analyses show that most (>80%) of the V is present as VO^{2+} ion, and Cr^{3+} is below detectable level (Table 1c). According to Mosser *et al.* (1996), VO^{2+} occurs within the octahedral sheet of the kaolinite structure (in the same way as Fe^{3+}). This is consistent with the presence of

V and VO^{2+} in the epithermal solution when the kaolinite formed. These authors also suggest that the V enrichment of initial hydrothermal fluid was probably derived from leaching of the V-rich titanomagnetites within the nearby sandstone deposit (Pacquet and Weber, 1993). Both the abundant pyrite (1.5%) associated with this kaolinite (Mosser *et al.*, 1996) and high V/Cr (7.1, Table 1c) indicates strong reducing conditions during the formation of the Cigar Lake kaolinite.

Hydrothermal dickites and kaolinites near Teslić. Maksimović *et al.* (1981) investigated three samples (herein referred as 2378, 664 and 665) of V- and Cr-bearing dickite and kaolinite from a hydrothermal sulfide vein in ultramafic rocks near Teslić (Bosnia). Samples 2378 and 665 contained predominantly dickite and kaolinite, respectively, while the third (664) contained equal proportions of both minerals. All three samples exhibited relatively high Cr and V (Table 1c). According to Maksimović *et al.* (1981), Cr occupies octahedral sites in the structures of these minerals. The authors suggested that the acidity of the hydrothermal solutions in which the dickite and kaolinite are formed was between pH 4.1 to 5.3 for a long period of time. They also reasoned that these pH conditions enhanced the geochemical separation of Cr and Al and enabled selective dissolution of Cr from the ultramafic source rocks. Low V/Cr ratios (≤0.2) (Table 1b) and the absence of sulfide minerals (*e.g.*, pyrite) associated with the Teslić dickite and kaolinite imply an oxygenated hydrothermal milieu.

The GB1 and Nopal hydrothermal kaolinites. GB1 is a primary, granite-hosted hydrothermal kaolinite. Our geochemical analysis indicates that the GB1 sample contains rather low concentrations (15 ppm) of V. VO^{2+} was not detected by ESR, and Cr was not detected by ICP-OES. The GB1 kaolinite formed under epithermal conditions (Malengreau *et al.*, 1994). The association of goethite with the GB1 kaolinite implies that the epithermal formation solution was oxygenated.

The Nopal kaolinite originated from hydrothermally altered ignimbritic (rhyolitic) tuffs (Muller *et al.*, 1990; Leslie *et al.*, 1993). Our geochemical analysis shows that the Nopal kaolinite sample contains 115 ppm of V, and that almost half (56%) of this V is in VO^{2+} form. Cr was not detected by ICP-OES. The formation of the Nopal kaolinite was epithermal with a temperature of about 360 K (Ildefonse *et al.*, 1990; Malengreau *et al.*, 1994).

Trace metal geochemistry (U, Th, REE) provides evidence for local mobilization of U under oxidizing conditions and further precipitation under reducing conditions. O- and H-isotope geochemistry of kaolinite (and other minerals) suggests that argillic alteration proceeded at shallow depth with meteoric water at about 300 – 375 °C (Calas *et al.*, 2008).

Hydrothermal V-rich kaolinite from the Rincon de la Vieja volcano. The near-surface hydrothermal pool system at the slope of Rincom de la Viejo volcano was formed by intense interaction of fluids enriched in sulfuric acids and rock wall materials. Detailed mineralogical analysis indicates that kaolinite is one of the major mineral phases and that it formed in a near-surface environment at temperatures between about 350-400 K. ESR investigation showed that VO^{2+} and Fe^{3+} are abundant in the kaolinite structure. This mineral formed under weakly oxygenated to oxygenated conditions (above 0.7 V) and at a pH as low as 4 (Gehring *et al.*, 1999).

CONCLUSION

From the results and considerations given in this paper the following conclusions can be drawn:

1) High concentrations of V (190 ppm) and Cr (435 ppm) were found in dickite.
2) High contents of VO^{2+} and Cr^{3+} were detected in dickite by ESR.
3) The V (and VO^{2+}) and Cr (Cr^{3+}) enrichments of dickite were probably occurred its formation by an invasive epithermal (acid-sulfate) solution.

4) The ultimate source of V and Cr in dickite was probably the surrounding gabbroic rocks of gabbro massifs of NR Basin.
5) V and Cr were leached by an initial hydrothermal (acid-sulfate) fluid before its mixing with a groundwater, forming an epithermal solution.
6) From the geochemistry of VO^{2+} and Cr^{3+}, it is deduced that the oxidation potential Eh and pH of the dickite-forming epithermal solution were >0.4 V and ≤4, respectively.

ACKNOWLEDGEMENTS

Funding support from le Ministere francais de l'Education National, del'Enseignement Superieur et de la Recherche to P. I. P. for his stay at Institut de Mineralogie et Physique des Milieux Condensés (IMPMC), Université Pierre et Marie Curie (Paris), is gratefully acknowledged. This work was supported in part by the Ministry of Science, Technology and Development (Serbia), Project 1235. Our thanks go to Drs. Jean-Pierre Girard and Adam Dangić who generously provided bibliographic material essential for writing this report. The English editing is done by American Journal Experts.

REFERENCES

Arehart, G.B. and Poulson, S.R. (2001) Hydrothermal systems as indicators of paleoclimate: an example from the Great Basin, western North America. *Proceedings of the 10th International Water-Rock Interaction Conference*, 87-90.

Balan, E., Allard, T., Morin, G. and Calas, G. (2002) Incorporation of Cr^{3+} in dickite: A spectroscopic study. *Physics and Chemistry of Minerals*, **29**, 273-279.

Beaufort, D., Cassagnabère, A., Petit, S., Lanson, B., Berger, G., Lacharpagne, J.C. and Johansen, H. (1998) Kaolinite-to-dickite conversion series in sandstone reservoirs. *Clay Minerals*, **33**, 297-316.

Bialowolska, A. (1973) Geochemistry of gabbro massifs of Nowa Ruda and Ślęża. *Archives of Mineralogy*, **31(1-2)**, 113-189.

Bigham, J.M., Schwertmann, U., Traina, S.J., Winland, R.L. and Wolf, M. (1996) Schwertmannite and the chemical modeling of iron in acid sulfate waters. *Geochimica et Cosmochimica Acta*, **60(12)**, 2111-2121.

Borkowska, M. (1985) Gabbroic rocks and their minerals from the Nowa Ruda massif (Sudetes). *Geological Sudetica*, **20(1)**, 3-35 (in Polish with English abstract).

Calas, G., Agrinier, P., Allard, T. and Ildefonse, P. (2008) Alteration geochemistry of the Nopal I uranium deposit (Sierra Peña Blanca, Mexico), a natural analogue for a radioactive waste repository in volcanic tuffs. *Terra Nova*, **20(3)**, 206-212.

Cassagnabère, A., Iden, I.K., Johansen, H., Lacharpagne, J.C. and Beaufort, D. (1999) Kaolinite and dickite in Frøy and Rind sandstone hydrocarbon reservoirs of the Brent Formation (Norwegian Continental Shelf). Pp. 97-102 in: *Clays of our Future*, *Proceedings of the 11th ICC* (H. Kodama, A. R. Mermut, and J. K. Torrance, editors). ICC97 Organizing Committee, Ottawa.

Davis, A., Chappell, R. and Olsen, R. (1988) The use and abuse of Eh measurements: Are they meaningful in natural waters? *Ground Water Geochemistry Conference 1988,* Dublin, Ohio, pp. 199-216.

DeLaune, R.D., Patrick, W.H.Jr. and Guo T. (1998) The redox-pH chemistry of chromium in water and sediment. Pp. 241-255 in: *Metals in Surface Waters III.* (H.E. Allen, A.W. Garrison and G.W. Luther, editors). Sleeping Bear Press, Chelsea.

Ehrenberg, S.N., Aagaard, P., Wilson, M.J., Fraser, A.R. and Duthie, D.M.L. (1993) Depth-dependent transformation of kaolinite to dickite in sandstones of the Norwegian continental shelf. *Clay Minerals*, **28**, 325-352.

Ehrenberg, S.N. and Nadeau, P.H. (1989) Formation of diagenetic illite in sandstones of the Garn formation, haltenbanken area, mid-Norwegian continental shelf. *Clay Minerals*, **24**, 233-253.

Evans H.T.Jr. (1978) Vanadium. In *Handbook of Geochemistry* (K.H. Wedepohl, editor). Springer-Verlag, Berlin. Vol II-2, Sect. 23-A.

Gaite, J.M., Ermakoff, P., Allard, T. and Muller, J.P. (1997) Paramagnetic Fe^{3+}: A sensitive probe for disorder in kaolinite. *Clays and Clay Minerals*, **45(4)**, 496-505.

Garrels, R.M. and Christ, C.L. (1965) *Solutions, Minerals and Equilibria*. Harper and Row, New York.

Gawroński, O. (1958) Szczegółowa Mapa Geologiczna Sudetów, arkusz Jugów (Detailed Geological Map of Sudetes Mts., sheet Jugów) 1: 25 000, Wydawnictwa Geologiczne.

Gehring, A.U., Schosseler, P.M. and Weidler, P.G. (1999) Mineral formation and redox-sensitive trace elements in a near-surface hydrothermal alteration system. *Geochimica et Cosmochimica Acta*, **63**, 2061-2069.

Goodman, B.A. and Raynor, J.B. (1970) Electron spin resonance of transition metal complexes.

Pp. 135-362 in: *Advances in Inorganic Chemistry and Radiochemistry* (H. J. Emeleus and A. G. Sharpe, editors) **13**, Academic Press, New York.

Hassouta, L., Buatier, M., Potdevin, J.L. and Liewig, N. (1999) Clay diagenesis in the sandstone reservoir of the Ellon field (Alwyn, North Sea). *Clays and Clay Minerals*, **47(3)**, 269-285.

Ildefonse, P., Muller, J.P., Clozel, B. and Calas, G. (1990) Study of two alteration systems as natural analogues for radionuclide release and migration. *Engineering Geology*, **29**, 413-439.

Izquierdo, G., Arellano, V.M., Aragón, A, Portugal, E. and Martinez, I. (2000) Fluid acidity and hydrothermal alteration at the Los Humeros geothermal reservoir Pubela, Mexico. *Proceedings of World Geothermal Congress 2000,* Kyushu – Tohoku, Japan, pp. 1301-1305.

Jones, B. and Manning, D.A.C. (1994) Comparison of geochemical indices used for the interpretation of palaeoredox conditions in ancient mudstones. *Chemical Geology*, **111**, 111-129.

Komusinski, J., Stoch, L. and Dubiel, S.M. (1981) Application of electron paramagnetic resonance and Mossbauer spectroscopy in the investigation of kaolinite-group minerals. *Clays and Clay Minerals*, **29**, 23-30.

Kowalski, W. M. and Lipiarski, I. (1973) Epithermal formations of the Słupiec syncline in the Sudetes basin. *Geological Transactions (Polska Akademia Nauk*, Warszawa), **78**, 7-71 (in Polish with English and Russian abstracts).

Kraynov, S.R. and Ryzhenko, B.N. (1992) Thermodynamic and kinetic aspects of systems controlling groundwater redox potentials. *Geochemistry International*, **29**, 1-8.

Krumbein, W.C. and Garrels, R.M. (1952) Origin and classification of chemical sediments in terms of pH and oxidation-reduction potential. *Journal of Geology*, **60**, 1-33.

Lahodny-Sarc, O., Dragcevic, Z. and Keller, W.D. (1993) The hydrothermal synthesis of kaolinite up to 350^{0}C. Pp. 325-341 in: *Kaolin genesis and utilization* (H. Murray, W. Bundy and

C. Harvey, editors). Special Publication, No. 1, Clay Mineral Society, Boulder.

Lanson, B., Beaufort, D., Berger, G., Baradat, J. and Lacharpagne, J.C. (1996) Late-stage diagenesis of clay minerals in porous rocks: Lower Permian Rotliegendes reservoir off-shore of The Netherlands. *Journal of Sedimentary Research*, **66**, 501-518.

Leslie, B.W., Pearcy, E.C. and Prikryl, J.D. (1993) Oxidative alternation of uraninite at the Nopal I deposit, Mexico: Possible contaminant transport and source term constraints for the proposed repository at Yucca Mountain. *MRS Symposium Proceeding*, **294**, 505-512.

Lydka, K. (1966) Dickite from Kamiensk near Walbrzych. *Archive of Mineralogy*, **26(1-2)**, 501-507 (in Polish with English abstract).

Maksimović, Z., White, J.L. and Logar, M. (1981) Chromium-bearing dickite and chromium-bearing kaolinite from Teslić, Yugoslavia. *Clays and Clay Minerals*, **29**, 213-218.

Malengreau, N., Muller, J.P. and Calas, G. (1994) Fe-speciation in kaolins: a diffuse reflectance study. *Clays and Clay Minerals*, **42,** 137-147.

McAulay, C.I., Fallick, A.E. and Hasezeldine, R.S. (1993) Textural and isotopic variations in diagenetic kaolinite from the Magnus oilfield sandstones. *Clay Minerals*, **28**, 625-639.

Moore, D.M. and Reynolds, R.C.Jr. (1989) Sample preparation techniques for clay minerals. Pp. 179-201 in: *X-ray Diffraction and the Identification and Analysis of Clay Minerals* (D.M. Moore and Jr. R.C. Reynolds, editors). Oxford University Press, Oxford and New York.

Morawiecki, A. (1956) Dickite and kaolinite veins (pholerites) from Nowa Ruda in Lower Silesia. *Biuletyn Instytutu Geologicznego Warszawa,* **103**, 5-56 (in Polish with English and Russian abstracts).

Mosser, C., Petit, S. and Mestdagh, M. (1993) ESR and IR evidence for chromium in kaolinites, *Clay Minerals*, **28**, 353-364.

Mosser, C., Boudeulle, M., Weber, F. and Pacquet, A. (1996) Ferriferous and vanadiferous kaolinites from the hydrothermal alteration halo of the Cigar Lake uranium deposit (Canada). *Clay Minerals*, **31**, 291-299.

Muller, J.P., Ildefonse, P. and Calas, G. (1990) Paramagnetic defect centers in hydrothermal kaolinite from an altered tuff in the Nopal Uranium deposit, Chihuahua, Mexico. *Clays and Clay Minerals*, **38**, 600-608.

Muller, J.P. and Calas G. (1993) Genetic significance of paramagnetic centers in kaolinites. Pp. 261-289 in: *Kaolin genesis and utilization* (H.H. Murray, W. Bundy and C. Harvey, editors). The Clay Mineral Society, Boulder.

Murray, H.H., Bundy, W. and Harvey, C. (1993) *Kaolin genesis and utilization.* The Clay Minerals Society, Special Publication 1.

Nicholson, K. (1993) *Geothermal Fluids. Chemistry and Exploration. Techniques.* Springer-Verlag, Berlin.

Oberc, J. (1960) Podział geologiczny Sudetów. Geological subdivision of the Sudetes. *Prace Panstwowy Instytut Geologiczny,* **30(2)**, 309-354 (in Polish).

Pacquet, A. and Weber, F. (1993) Pétrographie et minéralogie des halos d´altération autour du gisement de Cigar Lake et leurs relations avec les minéralisations. *Canadian Journal of Earth Sciences*, **30**, 674-688.

Premović, P.I. (1984) Vanadyl ions in ancient marine carbonaceous sediments. *Geochimica et Cosmochimica Acta*, **48**, 873-877.

Premović, P.I., Allard T., Nikolić, N.D., Tonsa, I.R. and Pavlović, M.S. (2000) Estimation of vanadyl porphyrin concentration in sedimentary kerogens and asphaltenes. *Fuel*, **79**, 813-819.

Rai, D., Sass, B.M. and Moore, D.A. (1987) Chromium(III) hydrolysis constants and solubility of chromium(III) hydroxide. *Inorganic Chemistry*, **26**, 345-349.

Rai, D., Zachara, J.M., Eary, L.E., Girvin, D.C., Moore, D.A., Resch, C.T., Sass, B.M. and Schmidt, R.L. (1986) Geochemical behavior of chromium species. *Interim Report* EPRI EA-4544, Electric Power Research Institute, Palo Alto, California.

Richard, F.C. and Bourg, A.C.M. (1991) Aqueous geochemistry of chromium: a review. *Water Research*, **25**, 807-816.

Ruiz Cruz, M.D. and Reyes, E. (1998) Kaolinite and dickite formation during shale diagenesis: isotopic data. *Applied Geochemistry*, **13**, 95-104.

Russell, J.D. (1987) Infrared methods. Pp. 133-173 in: *A Handbook of Determinative Methods in Clay Mineralogy* (M. J. Wilson, editor). Blackie, Glasgow.

Schroeder, J.B. and Hays, J.B. (1967) Dickite and kaolinite in Pennsylvania limestones of S. E. Kansas. *16th Clay Mineral Conference,* Denver. 29 (abstract).

Turekian, K.K. and Wedepohl, K.H. (1961) Distribution of the elements in some minor units of the earth's crust. *Geological Society of America Bulletin*, **72**, 175-190.

Turner, D.R., Whitfield, M. and Dickson, A.G. (1981) The equilibrium speciation of dissolved components in freshwater and seawater at 25°C and 1 atm pressure. *Geochimica et Cosmochimica Acta*, **45**, 855-881.

Wanty, W.B. and Goldhaber, M.B. (1992) Thermodynamics and kinetics of reactions involving vanadium in natural systems: Accumulation of vanadium in sedimentary rocks. *Geochimica et Cosmochimica Acta*, **56**, 1471-1483.

Watari, F., Delavignette, P., Van Landuyt, J. and Amelinckx, S. (1983) Electron microscopic study of dehydration transformations III. High resolution observation of the reactions process FeOOH-αFe_2O_3. *Journal of Solid State Chemistry*, **48**, 49-64.

Wehrli, B. and Stumm, W. (1989) Vanadyl in natural waters: Adsorption and hydrolysis promote oxygenation. *Geochimica et Cosmochimica Acta*, **53**, 69-77.

Whitfield, M. and Turner, D.R. (1987) The role of particles in regulating the composition of seawater. Pp. 457-493 in: *Aquatic Surface Chemistry* (W. Stumm, editor). J. Wiley & Sons, New York.

Wiewióra, A. (1967) Mineralogical and geochemical studies of weathering processes of gabroic rocks of the Nowa Ruda region (Lower Silesia). *Archive of Mineralogy*, **27(1)**, 245-360. (in Polish with English abstract).

Wójcik, L. (1956) Szczegółowa Mapa Geologiczna Sudetów, arkusz Nowa Ruda (Detailed Geological Map of Sudetes Mts., sheet Nowa Ruda) 1: 25 000, Wydawnictwa Geologiczne.

Table 1a. Geochemical distributions of V [ppm] and Cr [ppm] from selective leaching experiments of DS.

Fraction	Sediment (±5 wt%)	V	Cr
Acetate buffer	3	35	35
Cold-HCl	1	70	190
Boiling-HCl	3	40	340
Dickite*	91	190**	435
Insoluble residue	2	-	-
Total sample	100	175	410

*V/Cr = 0.4
**VO^{2+} concentration: 160 ± 20 ppm.

Table 1b. Geochemical distributions of V [ppm] and Cr [ppm] from selective leaching experiments of Jedlina dickite sample.

Fraction	Sediment (±5 wt%)	V	Cr
Acetate buffer	2	≤1	≤1
Cold-HCl	5	≤1	≤1
Boiling-HCl	2	≤1	50
Dickite*	91.5	≤1	≤1
Insoluble residue	0	-	-
Total sample	100.5	≤1	5

*This work.

Table 1c. Geochemical concentrations of V [ppm] and Cr [ppm] (on the whole-rock basis) in the Gey/Milo/Cigar Lake/Teslić samples.

Sample	V	Cr	V/Cr
Gey	320	23260	0.0
Milo	480	7530	0.1
Cigar Lake*	2475**	350	7.1
2378	190	4720	0.0
665	310	1780	0.2
664	230	3900	0.1

*This work.
**VO^{2+} concentration: 2700 ± 200 ppm.

Table 1d. Geochemical concentrations of V [ppm] and VO^{2+} [ppm] (on the whole-rock basis) in the GB1 and Nopal samples.

Sample	V	Cr	VO^{2+}
GB1	15	n.d.	n.d.
Nopal	115	n.d.	85

n.d. - not detected

FIGURE CAPTIONS

Fig. 1a. Simplified geological map of the dickite sampling area in NR Basin, modified after detailed Geological Map of Sudetes Mts, 1: 25 000, sheet Nowa Ruda, Wojcik, 1956 and sheet Jugów, Gawronski, 1958.

Fig. 1b. General stratigraphic section of NR region, modified after Morawiecki, 1956 and detailed Geological Map of Sudetes Mts, 1: 25 000, sheet Nowa Ruda, Wojcik, 1956 and sheet Jugów, Gawronski, 1958.

Fig. 2. Example of blue dickite filling the veins within black shales from the dump abandoned coal mine Piast. Sample size: 7 × 10 cm.

Fig. 3. Flow chart of fractionation procedure.

Fig. 4. FTIR spectra in the OH stretching vibrations zone of dickite.

Fig. 5. Scanning electron micrographs of the well- shaped dickite crystals.

Fig. 6. EDS spectrum of dickite.

Fig. 7. First derivative, room temperature, anisotropic VO^{2+} ESR spectrum of: untreated dickite (a); an initial glycerol solution containing 8000 ppm of VO^{2+} (b); and, a standard containing 400 ppm of VO^{2+} in the KGa-2/glycerol mixture (c).

Fig. 8. The glycerol/KGa-2 mixture as a standard for the VO^{2+} concentrations range from 50 to 400 ppm.

Fig. 9. First derivative, room temperature, anisotropic ESR spectrum of Cr^{3+} of untreated dickite: in low magnetic field region (a); and, high magnetic field region (b).

Fig. 10. Eh-pH diagram for VO^{2+} and Cr^{3+} at 300 K and 1 atm for formation of dickite. Total V concentration is 5 ppm. Probable physicochemical conditions of the epithermal solution are represented by the shaded area. The dashed line represents the Eh/pH region of the hydrothermal

waters defined by Kraynov and Ryzhenko (1992).

Fig. 11. The ESR spectrum of the untreated sample from Jedlina Zdroj with Fe^{3+} ions within the dickite structure.

Fig. 1a.

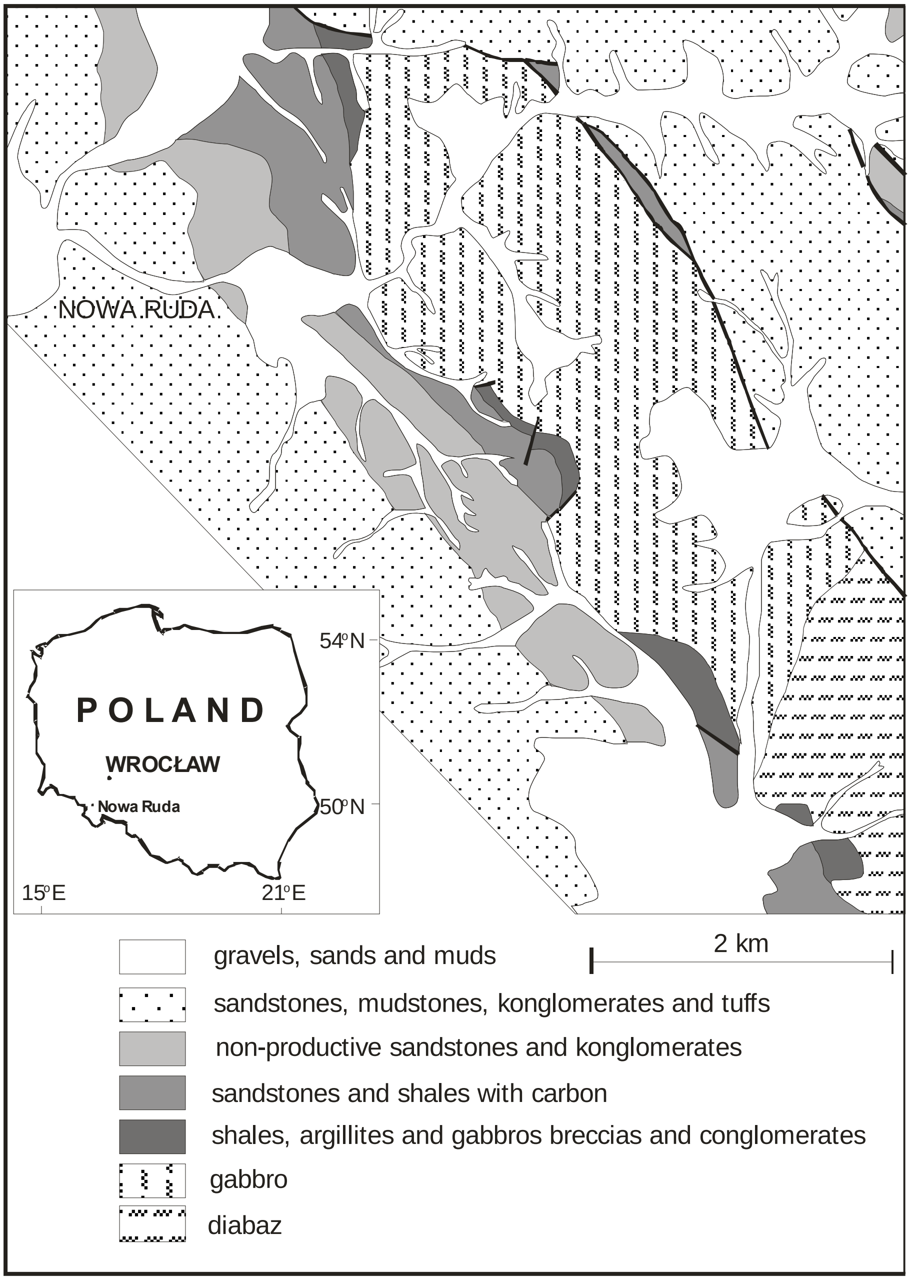
NOWA RUDA
POLAND
WROCŁAW
Nowa Ruda
54°N
50°N
15°E
21°E
2 km
gravels, sands and muds
sandstones, mudstones, konglomerates and tuffs
non-productive sandstones and konglomerates
sandstones and shales with carbon
shales, argillites and gabbros breccias and conglomerates
gabbro
diabaz

Fig. 1b.

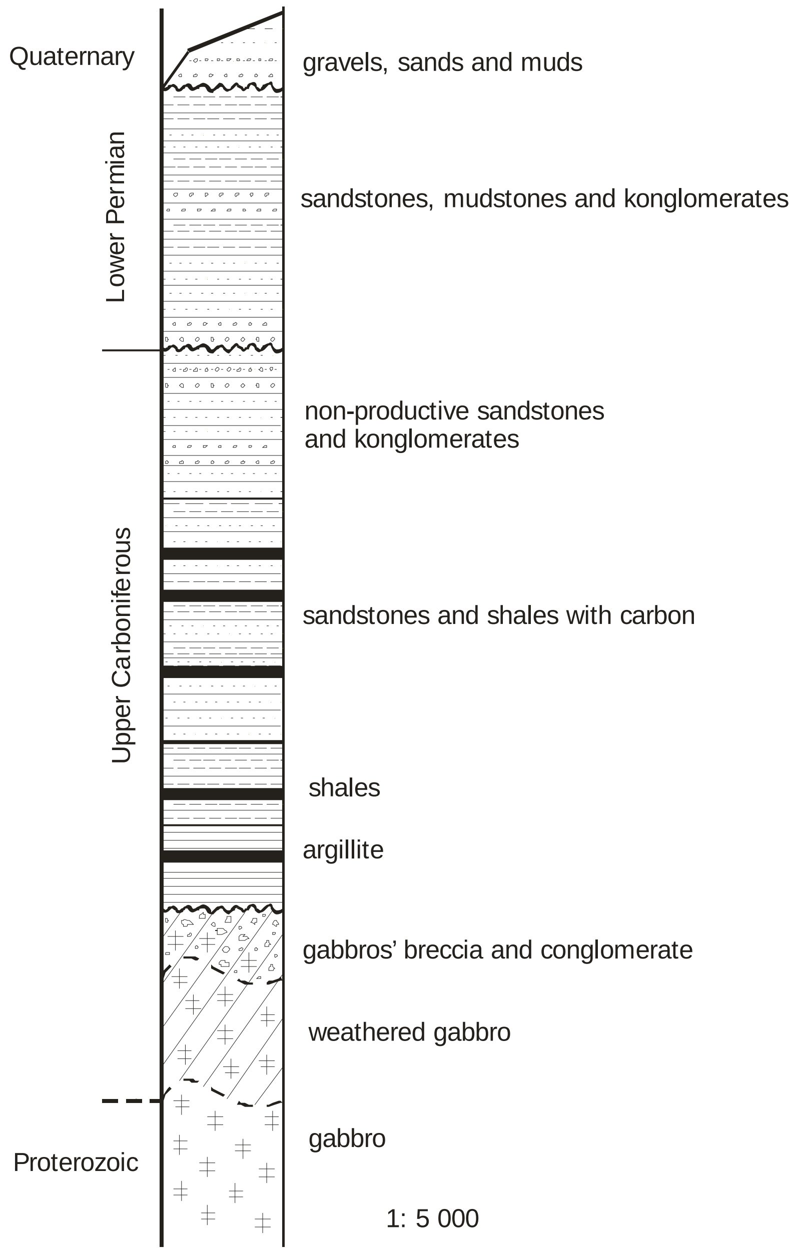
Quaternary
gravels, sands and muds
Lower Permian
sandstones, mudstones and konglomerates
non-productive sandstones
and konglomerates
Upper Carboniferous
sandstones and shales with carbon
shales
argillite
gabbros' breccia and conglomerate
weathered gabbro
gabbro
Proterozoic
1: 5 000

Fig. 2.

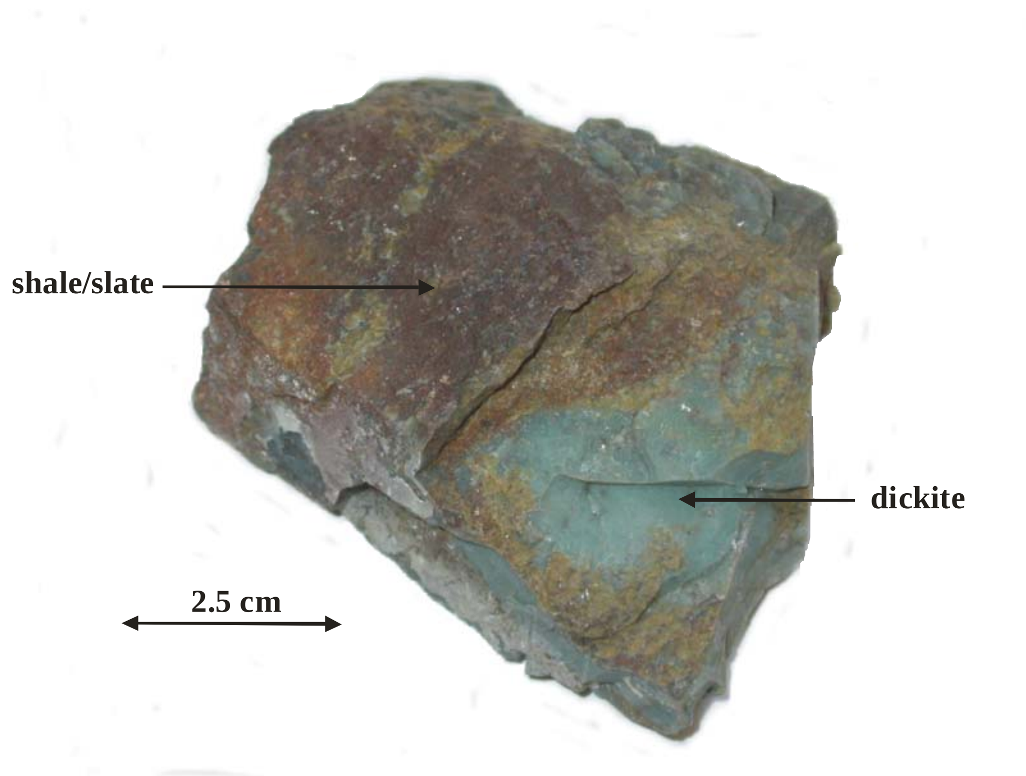

Fig. 3.

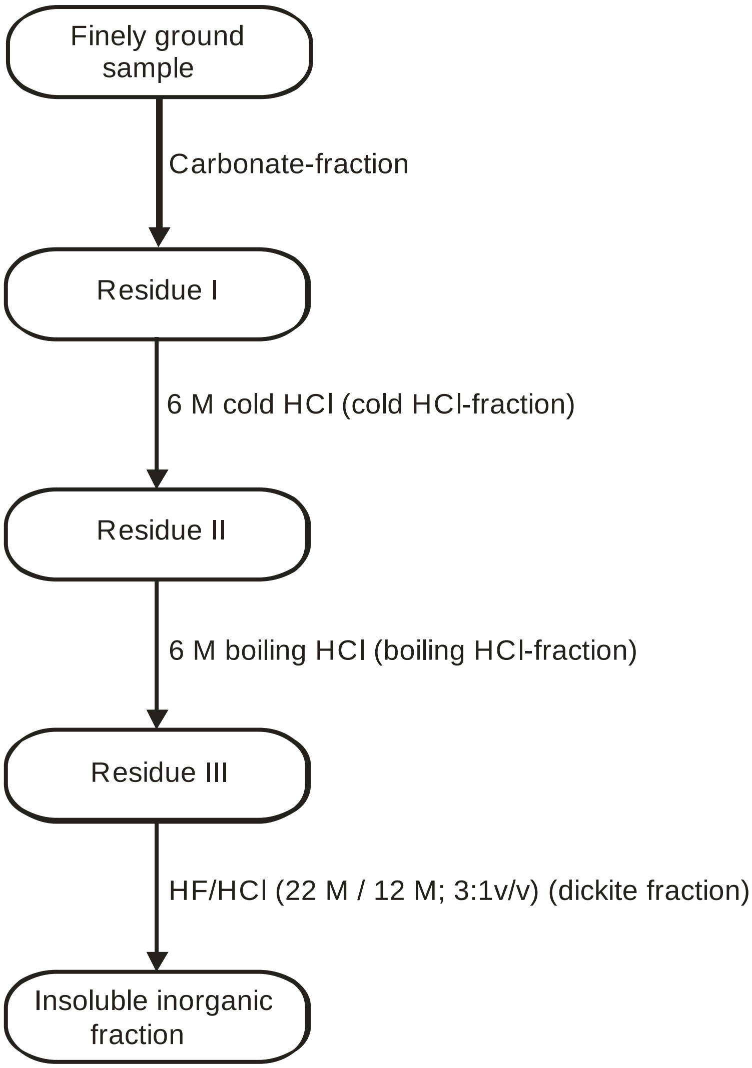

Finely ground sample
Carbonate-fraction
Residue I
6 M cold HCl (cold HCl-fraction)
Residue II
6 M boiling HCl (boiling HCl-fraction)
Residue III
HF/HCl (22 M / 12 M; 3:1v/v) (dickite fraction)
Insoluble inorganic fraction

Fig. 4.

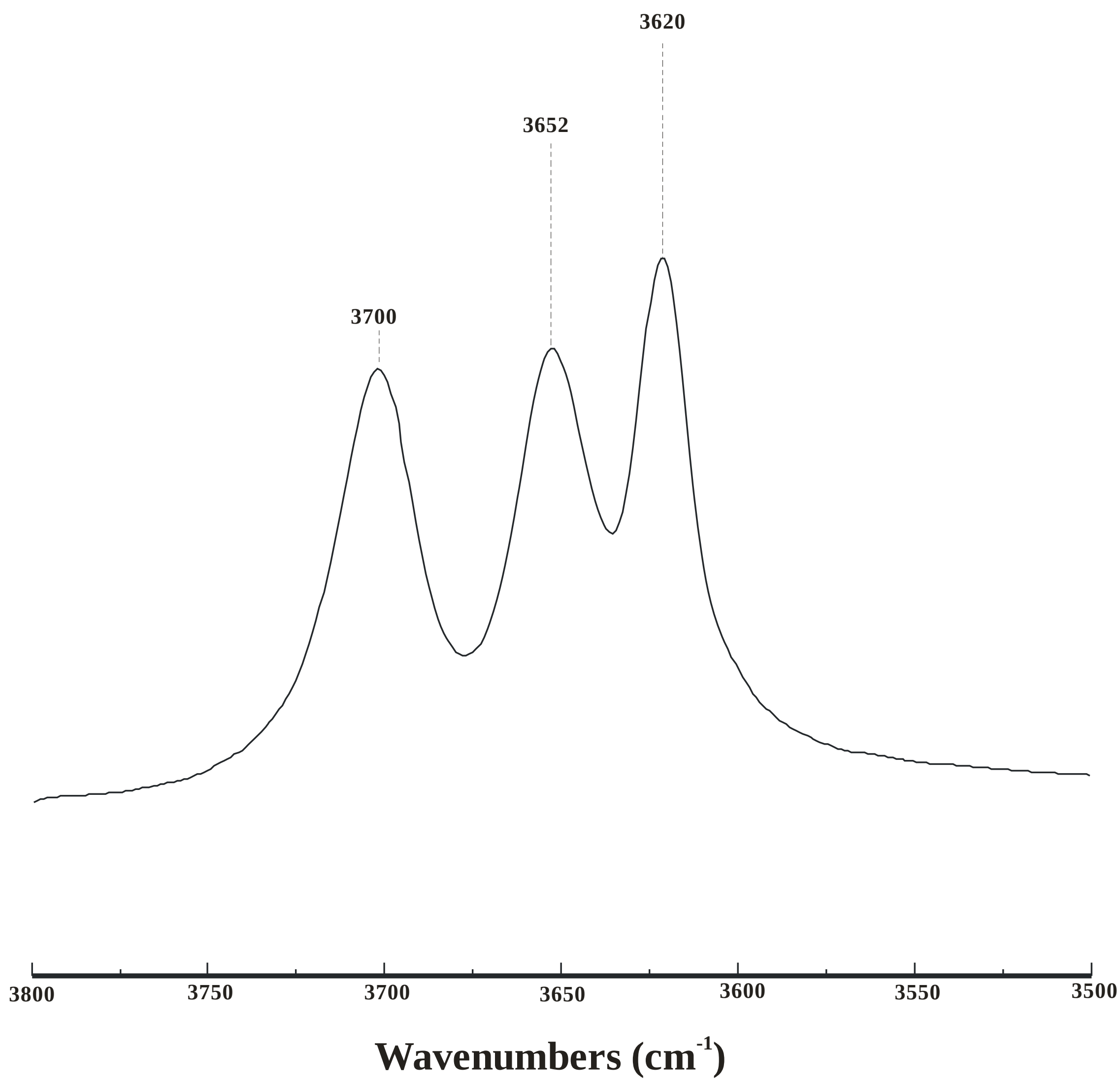

3620
3652
3700
3800
3750
3700
3650
3600
3550
3500
Wavenumbers (cm-1)

Fig. 5.

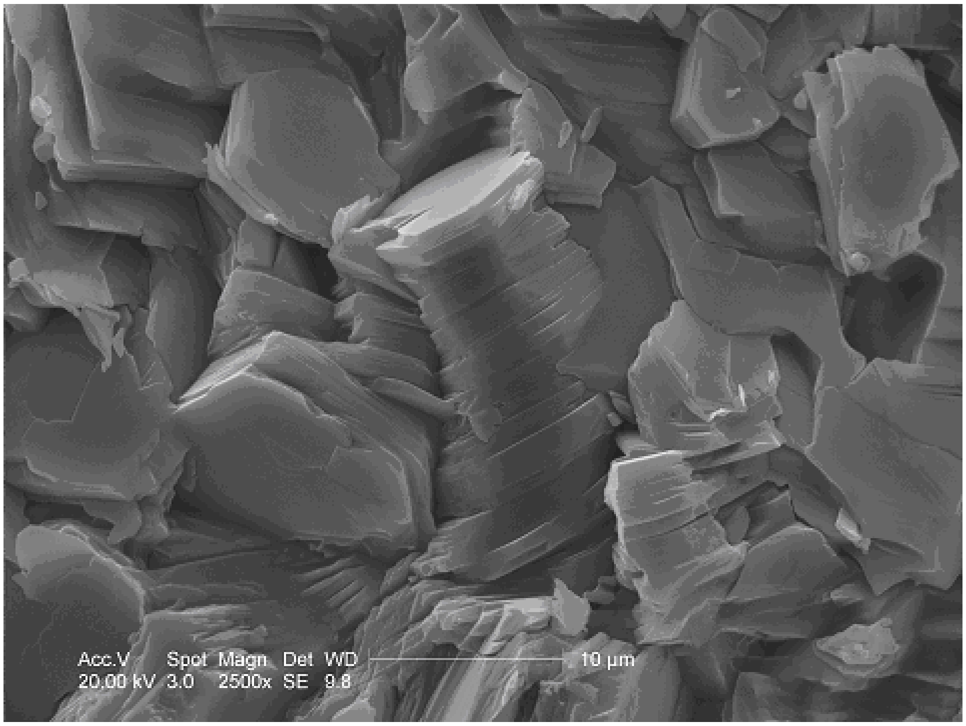

Fig. 6.

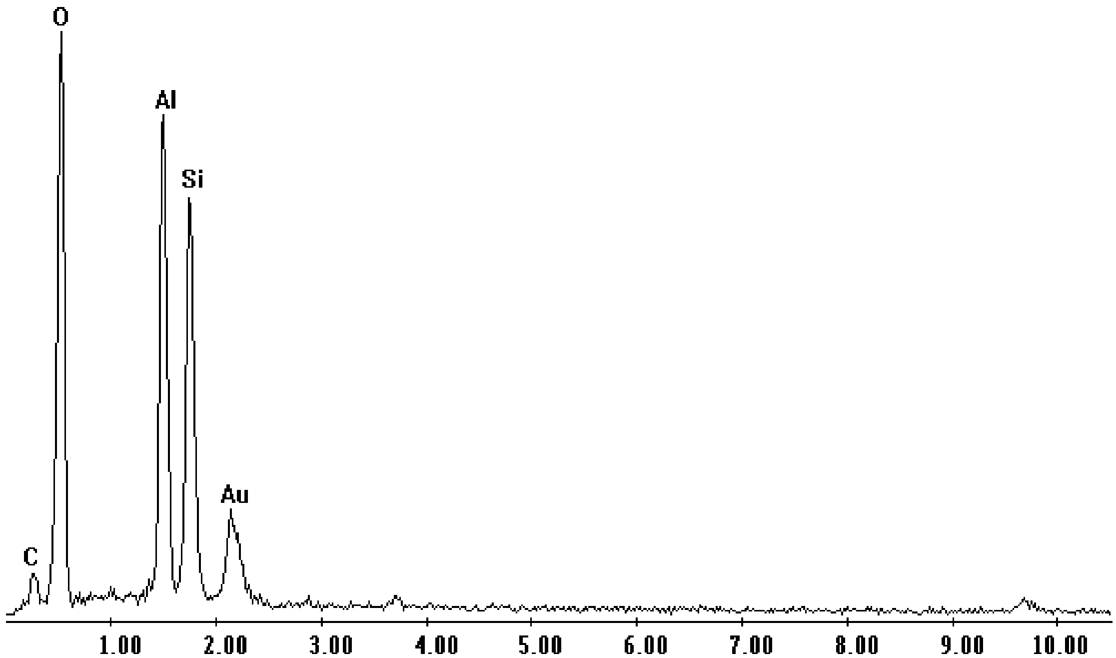

Fig. 7.

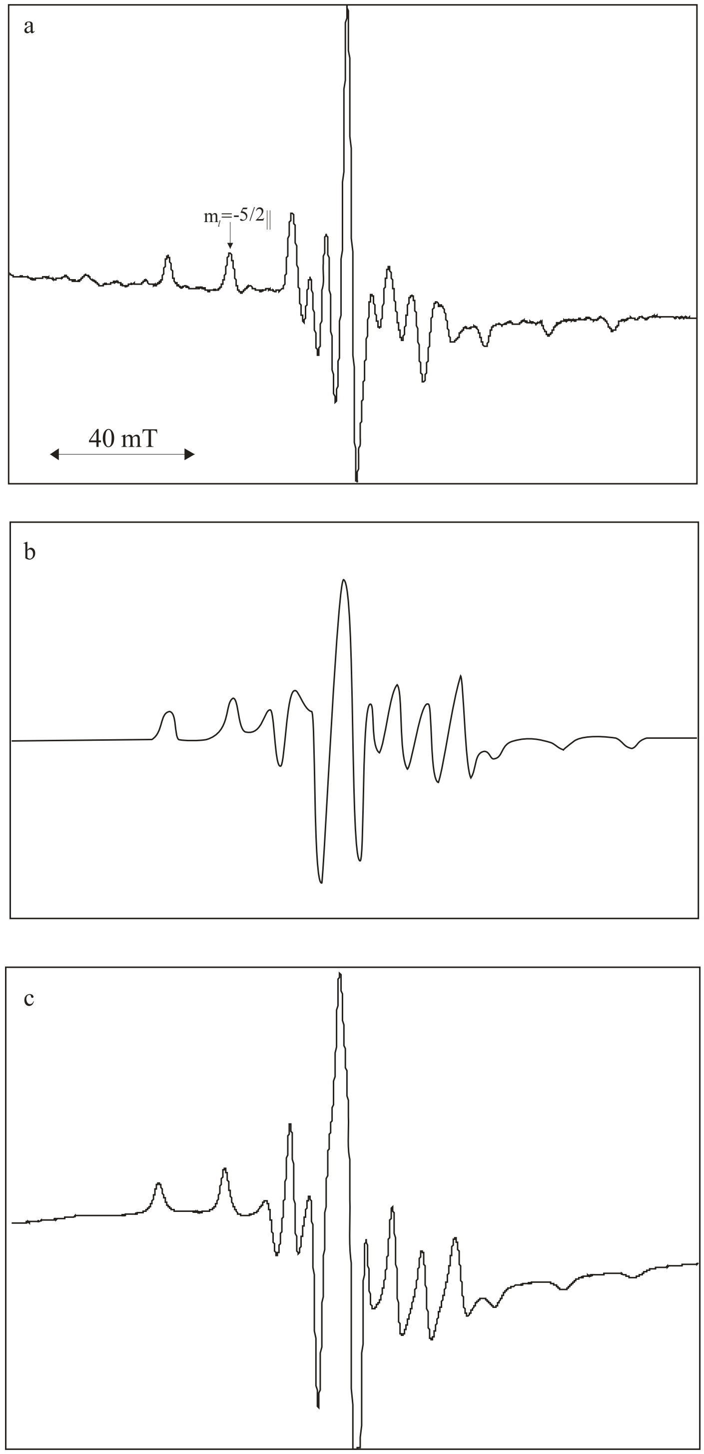

Fig. 8.

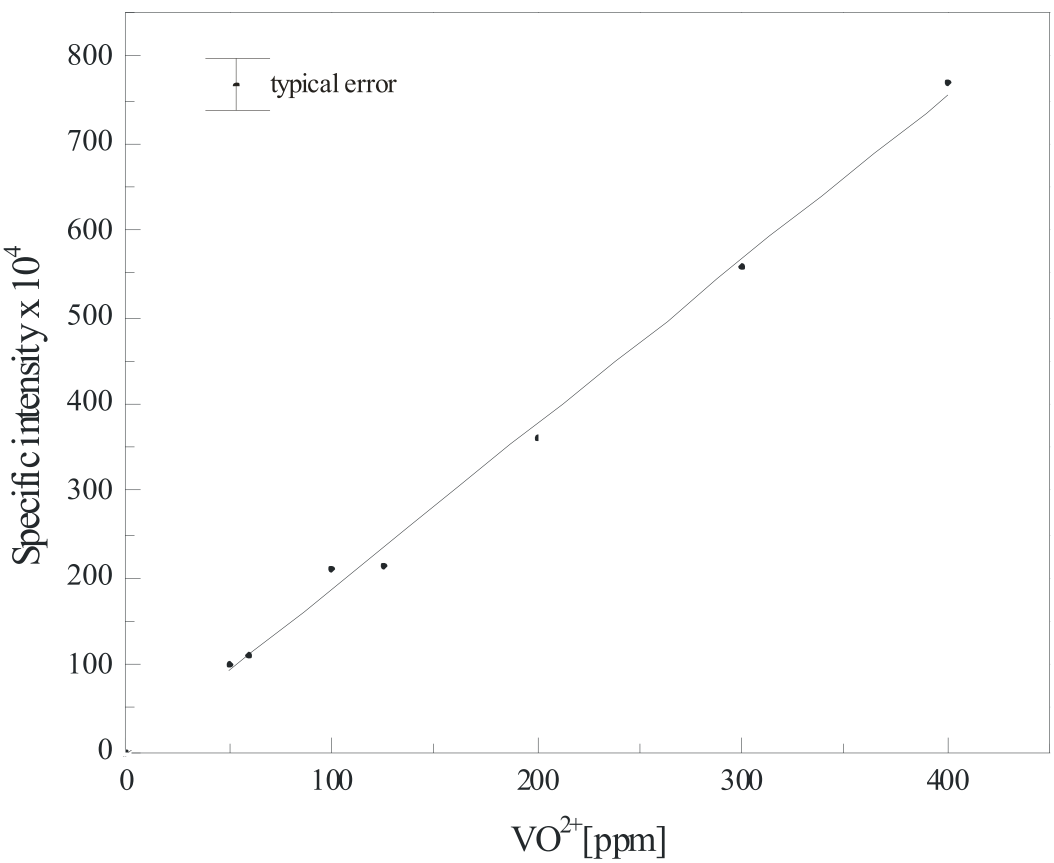

typical error
800
700
600
500
400
300
200
100
0
0
100
200
300
400
Specific intensity x 10^4
VO^{2+}[ppm]

Fig. 9.

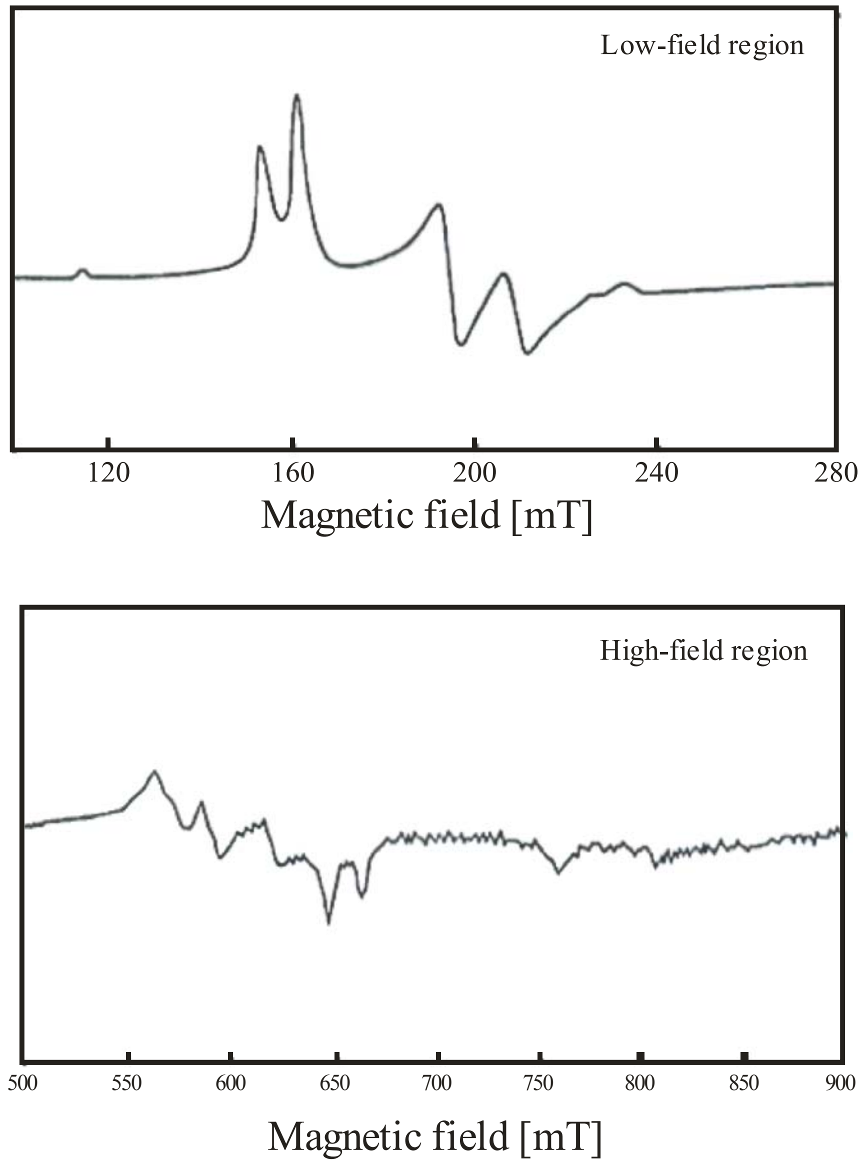
Low-field region
120
160
200
240
280
Magnetic field [mT]
High-field region
500
550
600
650
700
750
800
850
900
Magnetic field [mT]

Fig. 10.

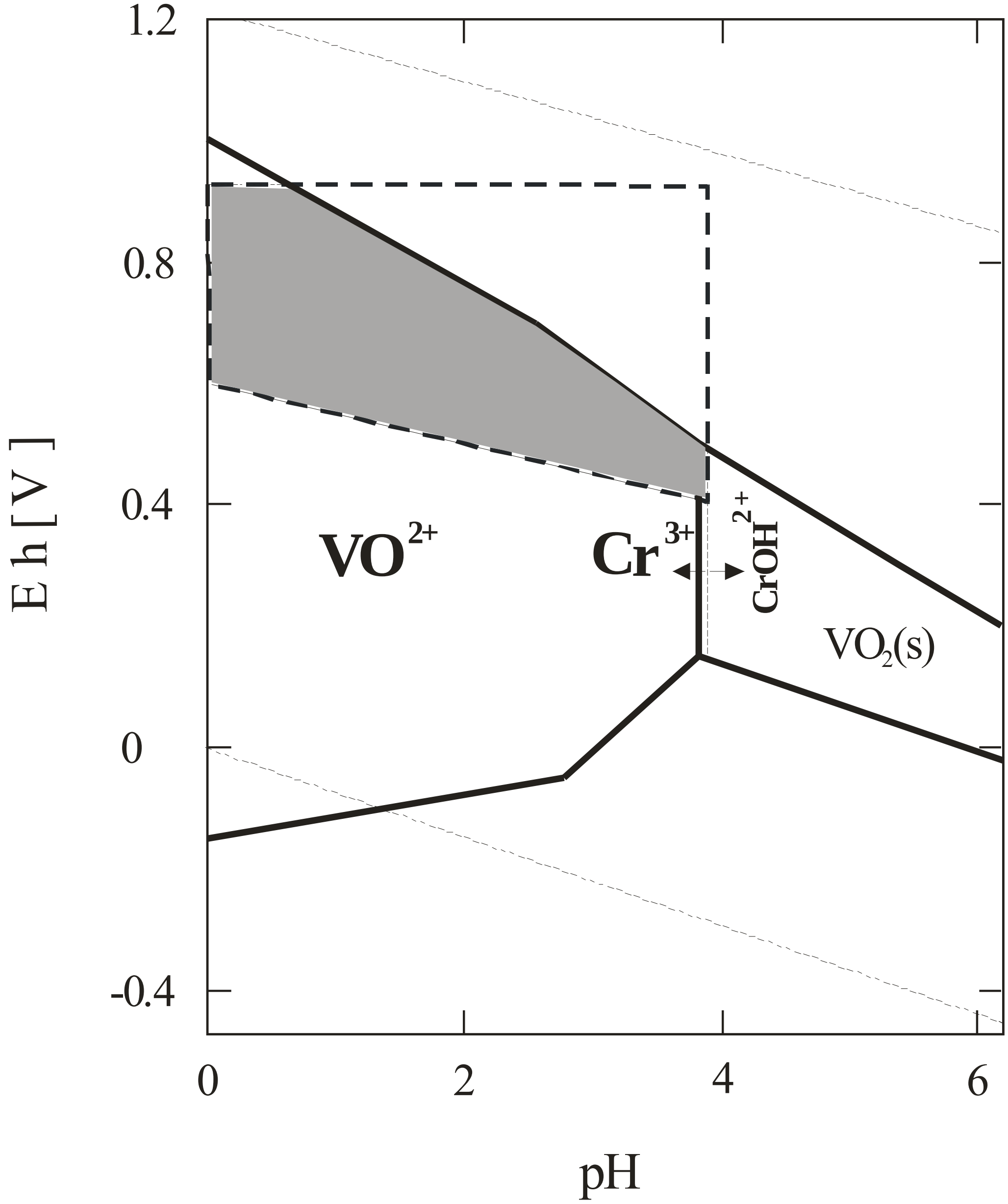

Fig. 11.